

ly circulating NNRTI-resistant strains in San Francisco pose a great and immediate threat to global public health.

References and Notes

- B. A. Larder, G. Darby, D. D. Richman, *Science* **243**, 1731 (1989).
- H. M. Truong *et al.*, *AIDS* **20**, 2193 (2006).
- S. M. Blower, H. B. Gershengorn, R. M. Grant, *Science* **287**, 650 (2000).
- J. Goudsmit *et al.*, *AIDS* **15**, 2293 (2001).
- A. Phillips, *Nat. Med.* **7**, 993 (2001).
- E. Tchetgen, E. H. Kaplan, G. H. Friedland, *J. Acquir. Immune Defic. Syndr.* **26**, 118 (2001).
- R. Vardavas, S. Blower, J. J. Miranda, *PLoS ONE* **2**, e152 (2007).
- G. S. Zaric, M. L. Brandeau, A. M. Bayoumi, D. K. Owens, *Simulation* **71**, 262 (1998).
- Materials and methods are available as supporting material on Science Online.
- C. L. Booth, A. M. Geretti, *J. Antimicrob. Chemother.* **59**, 1047 (2007).
- J. Martinez-Picado, M. A. Martínez, *Virus Res.* **134**, 104 (2008).
- L. Ross, N. Parkin, R. Lanier, *AIDS Res. Hum. Retroviruses* **24**, 617 (2008).
- S. Blower, H. Dowlatabadi, *Int. Stat. Rev.* **62**, 229 (1994).
- W. Lang *et al.*, *JAMA* **257**, 326 (1987).
- W. Winkelstein Jr. *et al.*, *JAMA* **257**, 321 (1987).
- J. K. Louie, L. C. Hsu, D. H. Osmond, M. H. Katz, S. K. Schwarcz, *J. Infect. Dis.* **186**, 1023 (2002).
- W. Lang, D. Osmond, K. Page-Bodkin, A. Moss, W. Winkelstein Jr., *J. Acquir. Immune Defic. Syndr.* **6**, 191 (1993).
- W. Lang *et al.*, *J. Acquir. Immune Defic. Syndr.* **4**, 713 (1991).
- J. C. Schmit *et al.*, *AIDS* **12**, 2007 (1998).
- J. J. Eron *et al.*, *N. Engl. J. Med.* **333**, 1662 (1995).
- C. Katlama *et al.*, *JAMA* **276**, 118 (1996).
- D. R. Kuritzkes, *AIDS Patient Care STDS* **18**, 259 (2004).
- B. S. Taylor, M. E. Sobieszczyk, F. E. McCutchan, S. M. Hammer, *N. Engl. J. Med.* **358**, 1590 (2008).
- A. J. Kandathil *et al.*, *Indian J. Med. Microbiol.* **27**, 231 (2009).
- R. M. Granich, C. F. Gilks, C. Dye, K. M. De Cock, B. G. Williams, *Lancet* **373**, 48 (2009).
- L. Breiman, J. H. Freidman, R. A. Olshen, C. J. Stone, *Classification and Regression Trees* (Chapman & Hall, Boca Raton, FL, 1984).
- C. Darwin, *The Origin of Species* (Signet, London, new ed. 1, 2003).
- K. A. Powers, C. Poole, A. E. Pettifor, M. S. Cohen, *Lancet Infect. Dis.* **8**, 553 (2008).
- S. M. Hammer *et al.*, *JAMA* **300**, 555 (2008).
- R.J.S., J.T.O., E.N.B., and S.B. acknowledge the financial support of the National Institute of Allergy and Infectious Diseases (NIAID) (R01 AI041935). R.J.S. is supported by a Natural Sciences and Engineering Research Council of Canada discovery grant, an Early Researcher award, and funding from Mathematics of Information Technology and Complex Systems. In addition, S.B. acknowledges the John Simon Guggenheim Foundation, the National Academies Keck Foundation, and the Semel Institute for Neuroscience & Human Behavior. J.S.K. acknowledges NIAID grants P30-AI27763, NCRK K24RR024369, and AHRQ R18-HS017784. We thank R. Breban, D. Freimer, J. Freimer, N. Jewell, E. Kajita, T. Pytko, V. Supervie, and R. Vardavas for useful discussions throughout the course of this research.

Supporting Online Material

www.sciencemag.org/cgi/content/full/science.1180556/DC1

Materials and Methods

Figs. S1 to S6

Tables S1 to S13

References

13 August 2009; accepted 16 December 2009

Published online 14 January 2010;

10.1126/science.1180556

Include this information when citing this paper.

Optimal Localization by Pointing Off Axis

Yossi Yovel,¹ Ben Falk,² Cynthia F. Moss,² Nachum Ulanovsky^{1*}

Is centering a stimulus in the field of view an optimal strategy to localize and track it? We demonstrated, through experimental and computational studies, that the answer is no. We trained echolocating Egyptian fruit bats to localize a target in complete darkness, and we measured the directional aim of their sonar clicks. The bats did not center the sonar beam on the target, but instead pointed it off axis, accurately directing the maximum slope (“edge”) of the beam onto the target. Information-theoretic calculations showed that using the maximum slope is optimal for localizing the target, at the cost of detection. We propose that the tradeoff between detection (optimized at stimulus peak) and localization (optimized at maximum slope) is fundamental to spatial localization and tracking accomplished through hearing, olfaction, and vision.

Most sensory systems allow some active control over the information acquired from the environment (1–6). Nowhere is this more evident than in echolocating bats (4, 7–10), which control many aspects of their sonar signal design (4, 7, 9, 11–16) and use returning echoes to orient and forage in the dark (4, 7–16). We trained Egyptian fruit bats to fly in a large flight room and land on a spherical target while relying exclusively on sonar (17). The bats’ three-dimensional (3D) position was measured with two infrared cameras, and the shape and direction of their sonar beam pattern were measured with a 20-microphone array (17) (Fig. 1, A to D, and movie S1).

At the beginning of each trial, the target was randomly repositioned. Subsequently, the bat

sought for the target, approached it, and landed on it, either by a straight flight or a curved trajectory (Fig. 1C and fig. S1). Unlike microbats (microchiropteran bats), which emit laryngeal tonal calls, Egyptian fruit bats are megabats (megachiropteran bats) that produce very short (50- to 100- μ s) impulse-like tongue clicks, with frequencies centered at 30 to 35 kHz (fig. S2). While flying, bats typically emitted pairs of clicks, with an \sim 20-ms interval within the click pair and an \sim 100-ms interval between the pairs (Fig. 1A and fig. S3) (18, 19). The bats pointed their sonar beam toward the left or the right, in an alternating manner as follows: left \rightarrow right \rightarrow 100-ms interval \rightarrow right \rightarrow left (Fig. 1D and movie S1).

We observed two different phases of behavior. During the first stage, the bats did not necessarily lock their click pairs onto the target, and the directions of clicks were widely distributed (the “unlocked” phase). At the final stage, the bats directed their sonar clicks so that the vector average of the pair of clicks pointed toward the target with accuracy better than 30°

(17). We refer to this as the “locked” phase (Figs. 1E, arrows, and 2A, top, and fig. S1C). During this phase, 0.5 s before landing, 80% of the click pairs were locked with accuracy better than 15° (Fig. 2A, bottom, gray lines). In 10% of the trials, the bats locked onto the target with average accuracy better than 5°. The left-right orientation of the clicks in the locked phase implies that the bats did not direct the maximum intensity of the click toward the target, contradicting the common notion that bats steer their sonar beam in order to maximize the signal-to-noise ratio (SNR) of the echoes (13, 20).

Another possible strategy would be for the bats to direct the maximal slope of the beam’s emission curve toward the target, because this would maximize changes in reflected echo energy that result from changes in the relative position of the bat and the target. Plotting the directional span of the beams between the right and left maximum slope (green lines in Fig. 1, E and F, and fig. S1, C and D) showed that the bats consistently placed the maximum slope of their beams onto the target (Fig. 1F and fig. S1D; the top and bottom of the green lines are close to direction 0°). Next, we examined the population distribution of the directions of the beams’ maximum intensity and maximum slope (Fig. 2, B and C, top two rows). Before locking, the bats directed their sonar beams over a wide range of angles, spanning $>100^\circ$ around the target (Fig. 2B, top). After locking, however, they clearly directed their beam so that the maximum slope of the intensity curve of the beam, and not its peak, was on the target (Fig. 2C, middle row). All six bats exhibited this behavior (fig. S4).

When the maximum slope of the beam is directed toward an object, any motion of the object relative to the bat will result in the largest possible change in echo intensity. The sign of the energy change (positive or negative) corresponds to the

¹Department of Neurobiology, Weizmann Institute of Science, Rehovot 76100, Israel. ²Department of Psychology, Institute for Systems Research and Neuroscience and Cognitive Science Program, University of Maryland, College Park, MD 20742, USA.

*To whom correspondence should be addressed. E-mail: nachum.ulanovsky@weizmann.ac.il

direction of motion. We hypothesized that Egyptian fruit bats lock the maximum slope on the target as a strategy that maximizes their sensitivity to changes in target azimuth, in order to better localize the target.

To test this “optimal-localization” hypothesis, we used the Fisher information (FI) measure that is commonly used to assess sensitivity to small differences (21). To estimate the FI at different angles relative to the target, we computed joint probability-density functions of the intensities and angles for all clicks (17). After locking, the beam-steering strategy used by the bats maximized the FI in the direction of the target (Fig. 2C, bottom row). There is a secondary peak in the FI curve, because each emission curve has two points of maximum slope (one on each side). The secondary peak is higher because of the inherent asymmetry of the beam (Fig. 3A). Because the FI is a measure that meets a theoretical optimality criterion (21), this result implies that the strategy used by the bats is optimal for localizing the target based on the intensity of reflected echoes.

We ruled out an alternative explanation for the bats’ behavior, namely that they might have placed the peaks of the beams on the target’s edges. In this case, we would expect the angle between the pair of clicks to increase as the bat approaches the target, because the angular extent of the target increases. However, we found no such increase in angle (fig. S5).

This optimal-localization strategy is not free of cost. When pointing the maximum slope of the emission curve and not its peak toward an object, less energy (6 dB) is reflected back from the object (Fig. 3, A and B), and this reduces object detectability, decreasing the maximal detection range by ~16% (17). We hypothesize, therefore, that the part of the beam between the peak and the maximum slope of the emission curve can be used by bats to trade off between detection and localization. The beam’s peak provides optimal detection, whereas the maximum slope provides optimal localization. The bat could direct the beam according to the task, target properties, or ambient noise. Bats landing on an acoustically salient object, as in our experiments, preferred to maximize spatial localization in order to land accurately. A bat confronted by a detection problem, such as a small target, a noisy environment, or a strong masker, should act to maximize detection by placing the beam’s peak on the target (22). A bat that needs both detection and localization will have to compromise between the two positions on the emission curve (Fig. 3B). Indeed, the area between the peak and the slope was directed toward the target more often than the area beyond the slope, which is consistent with a detection-localization compromise [Fig. 2C, top; the peak’s distributions are significantly skewed toward the target at angle 0°; *t* test: $\gamma_{\text{right}} = -0.42$, $P < 0.001$; $\gamma_{\text{left}} = 0.26$, $P < 0.001$ (17)].

To further test this “detection-localization tradeoff” hypothesis, we conducted a control experiment in which a large reflecting board was positioned 50 to 80 cm behind the target (17). Such a reflector returns strong echoes that arrive shortly after the target’s echo, thus acting as a powerful acoustic masker that interferes with target detection. Indeed, some bats changed their beam-steering strategy; initially they maintained the left→right→right→left pattern as described above, but then, in the final approach (~1 s before landing), they directed both clicks of each click pair forward and pointed at the target a part of the emission curve that was close to the beam’s peak (Fig. 3C, bottom, black dots, and fig. S6). This switch in strategy was exhibited by bats that chose to fly directly toward the target. It should increase echo energy and improve detection (improve SNR). The bats’ flexibility in steering their emission beams suggests that in our main experiments (Figs. 1 and 2), the animals actively chose to direct the maximum slope of the beam toward the target.

It remains an open question whether other echolocating animals (microbats, dolphins, swiftlets, etc.) use the maximum-slope strategy for localizing objects. All studies that tested beam steering in microbats (13, 20, 23) did so in the context of small targets, which created a detection problem. We predict that, when localization is paramount and detection is not challenged, microbats would also use the slope-based optimal-localization

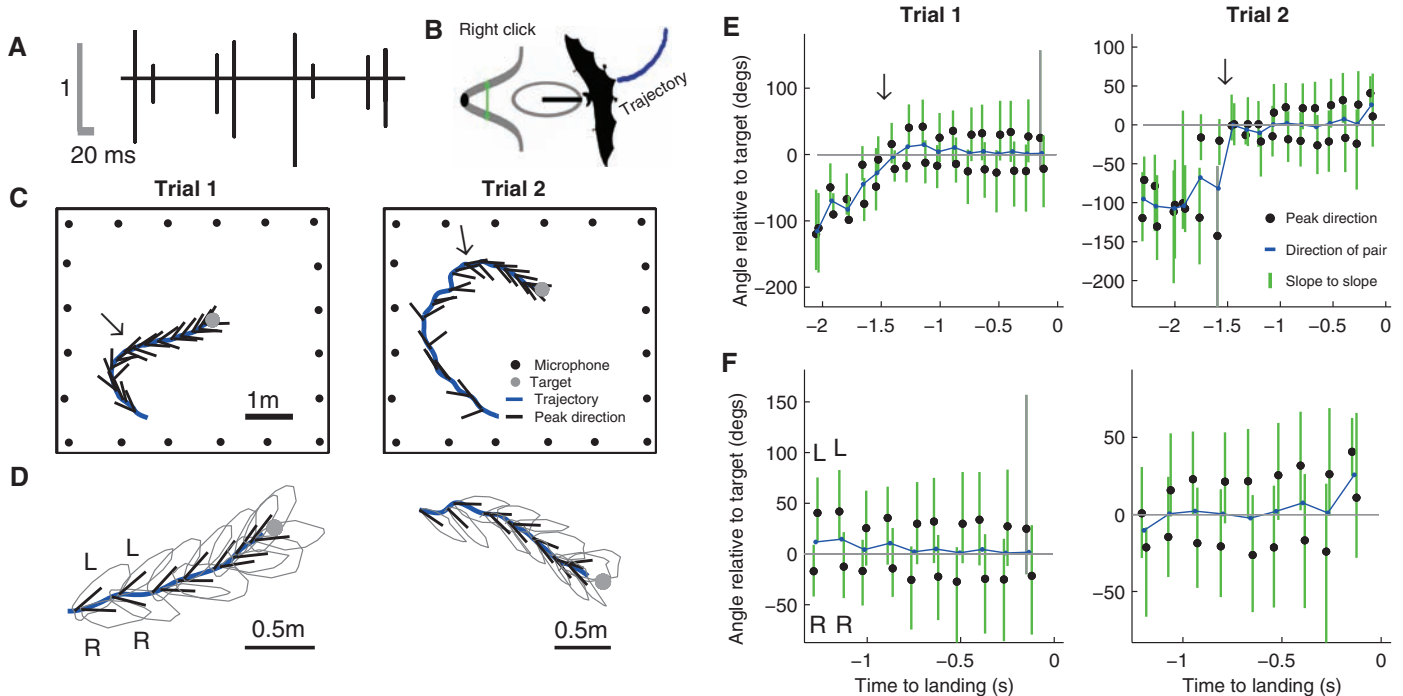


Fig. 1. Examples of flight and echolocation behavior. (A) Representative time signal showing four click pairs. The y axis shows signal amplitude (on a linear scale, with the largest excursion normalized to 1). (B) Schematic of bat emitting a right click. Ellipse, sonar beam in polar coordinates; Gaussian curve, sonar beam in Cartesian coordinates; black dot, peak intensity. The green line connects the two points of maximum slope. (C to F) Examples of two behavioral trials. (C) Top view of the room. Blue line, bat’s flight trajectory; short black lines, sonar beam directions for all clicks; arrow, point of

locking onto target. (D) Close-up on locked part of the trials in (C); same notation as in (C). Gray curves, polar representation of the beams (dB scale). (E) Diagrams of beam angles relative to the target for the same two trials. Green lines connect the beam’s right and left maximum slope. Gray lines, clicks that did not meet the inclusion criteria (17); black dots, direction of beam’s peak; blue line, average direction of each pair of black dots; arrows, point of locking. (F) Close-up on the locked part of (E); same notation as in (E). The bats tended to place the maximum slope (end of green lines) onto the target.

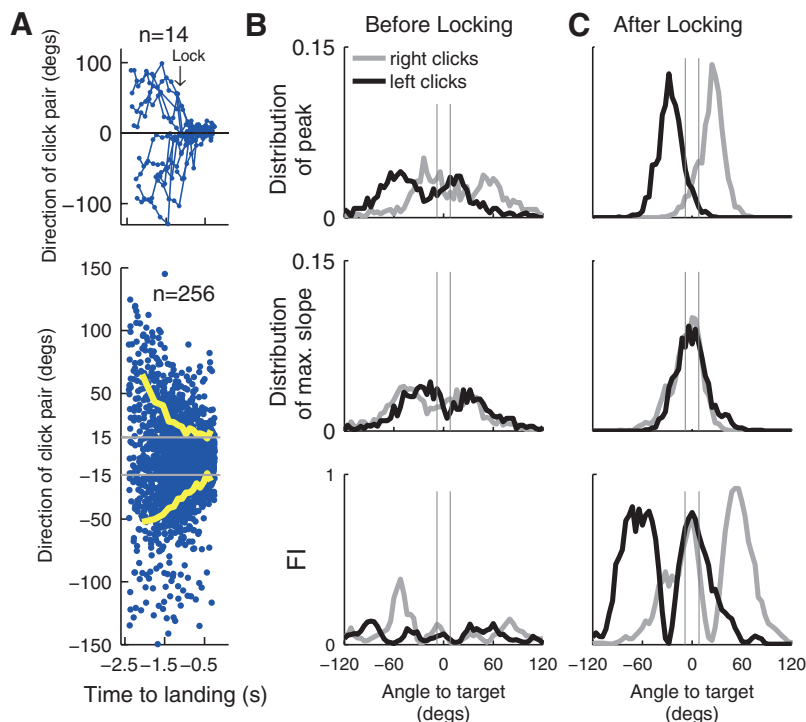
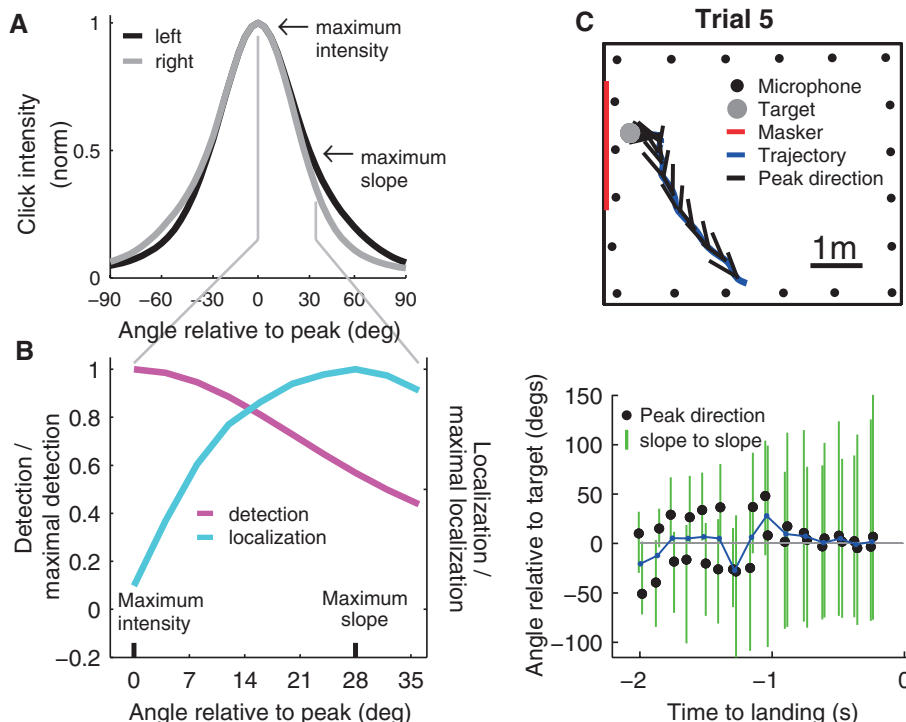


Fig. 2. Population analysis shows that bats optimize angular localization by locking the maximum slope of the beam onto the target. **(A)** Top: Direction of click pair (vector average) relative to the target as function of time to landing for 14 example trials. Blue lines, same notation as blue lines in Fig. 1E; black arrow, average time of locking onto target. Bottom: The same for all 256 trials. Yellow lines, mean \pm SD, computed in 100-ms windows; gray lines, $\pm 15^\circ$. **(B and C)** Directional distributions of click parameters and FI relative to target direction, **(B)** before locking and **(C)** after locking. Top: distribution of the direction of the beam's peak intensity. Middle: distribution of the direction of the beam's maximum slope. Bottom: FI as function of angle to target. Gray vertical lines, $\pm 5.5^\circ$ total error in estimating bat/object directions (17). The y axes are identical in **(B)** and **(C)**.

Fig. 3. The tradeoff between detection and angular localization. **(A)** Average left click and right click (averaged across all locked clicks of all bats). The emission curve is asymmetric (less steep on the side directed toward the target). This explains the higher secondary peaks in the FI curve (Fig. 2C, bottom). **(B)** Detection-localization tradeoff for the biosonar of Egyptian fruit bats. Magenta, detection (in normalized units); cyan, localization (azimuthal discriminability, d'). The x axis shows the angle within the emission beam, shown between the peak and 36° . The localization accuracy decreases beyond the maximum slope. **(C)** Example of flight trajectory and echolocation behavior for one trial from the masker experiments (detection problem). Top and bottom, same notations as in Fig. 1, C and E, respectively; red line, masker. Approximately 1 s before landing, the bat switched from a left-right maximum-slope strategy to a peak strategy (black dots).

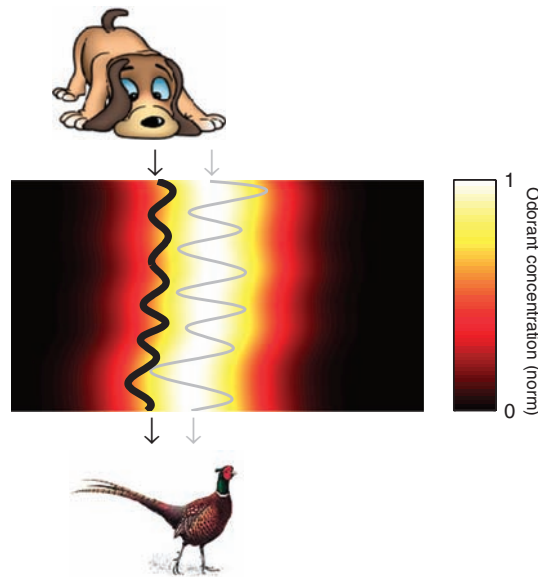


strategy; however, because microbat biosonar is based on single pulses instead of double clicks (4, 7–10), the microbats would always place one of the beam's slopes on target (for example, right→right→right...) and analyze echo-amplitude changes between successive calls. The mechanism by which Egyptian fruit bats direct their beams left→right is not entirely clear [supporting online material (SOM) text], but the alternating clicks of these megabats are certainly advantageous in that comparing two different slopes doubles the intensity difference.

Previous neurophysiological studies in microbats have reported auditory neurons tuned to echo amplitude (24). Our results point to the possibility that, in megabats, upstream of such echo-amplitude-tuned neurons, there might be neurons that are sensitive to the amplitude difference of two successive echoes (20 ms apart). In both microbats and megabats, the directional accuracy of passive hearing is 10° to 15° (25), whereas active mechanisms, such as described here, could underlie the improved accuracy of 1.5° to 5° during active echolocation (12, 20).

We further hypothesize that the tradeoff between detection (SNR) and localization is a general dilemma in sensory systems. If we describe the intensity of a stimulus (for example, olfactory or visual) as a contour in space, its peak would be optimal for detection, but the maximum slope is optimal for spatial localization. For example, we predict that an organism following an odor trail should follow the line of the maximum slope of the odor concentration in order to optimize the tracking accuracy and minimize movement jitter (Fig. 4). A study that measured odorant spatial distribution in an

Fig. 4. Prediction for other sensory systems (olfaction). Color map, schematic odor trail; gray line, path of an organism that followed the trail's peak concentration. This strategy is typically assumed for odor-trail following (3). Black line, path of the same organism when using a strategy similar to that of our bats, that is, following the maximum slope of the odorant concentration (17). The movement jitter in this case is smaller, making the tracking smoother and therefore faster.



olfactory-tracking task indicated that *Drosophila* larvae seem to follow a trajectory between the peak and the maximum slope (26). Similarly, in the case of vision, we predict that when tracking large moving objects, humans would place their fovea on the object's intensity slope to optimize tracking. Finally, several recent studies have reported sensory neurons that best encode stimulus location via the maximum slope of their tuning curve (22, 27–29), not via the peak firing rate of the tuning curve. Such coding maximizes the discriminability of the on-slope stimulus, paralleling our behavioral results, which show an optimal-localization strategy at the sensor's behavioral level.

References and Notes

1. D. Kleinfeld, E. Ahissar, M. E. Diamond, *Curr. Opin. Neurobiol.* **16**, 435 (2006).
2. K. C. Catania, *Nature* **444**, 1024 (2006).
3. J. Porter *et al.*, *Nat. Neurosci.* **10**, 27 (2007).
4. N. Ulanovsky, C. F. Moss, *Proc. Natl. Acad. Sci. U.S.A.* **105**, 8491 (2008).
5. M. E. Nelson, M. A. MacIver, *J. Comp. Physiol. A* **192**, 573 (2006).
6. W. W. Au, K. J. Benoit-Bird, *Nature* **423**, 861 (2003).
7. G. Jones, M. W. Holderied, *Proc. Biol. Sci.* **274**, 905 (2007).
8. H.-U. Schnitzler, C. F. Moss, A. Denzinger, *Trends Ecol. Evol.* **18**, 386 (2003).
9. J. A. Simmons, M. B. Fenton, M. J. O'Farrell, *Science* **203**, 16 (1979).
10. N. Suga, *J. Exp. Biol.* **146**, 277 (1989).
11. W. Metzner, *Nature* **341**, 529 (1989).
12. W. M. Masters, A. J. Moffat, J. A. Simmons, *Science* **228**, 1331 (1985).

13. K. Ghose, C. F. Moss, *J. Neurosci.* **26**, 1704 (2006).
14. N. Ulanovsky, M. B. Fenton, A. Tsoar, C. Korine, *Proc. Biol. Sci.* **271**, 1467 (2004).
15. C. Chiu, W. Xian, C. F. Moss, *Proc. Natl. Acad. Sci. U.S.A.* **105**, 13116 (2008).
16. E. K. V. Kalko, H.-U. Schnitzler, *Behav. Ecol. Sociobiol.* **33**, 415 (1993).
17. Materials and methods are available as supporting material on Science Online.
18. R. A. Holland, D. A. Waters, J. M. Rayner, *J. Exp. Biol.* **207**, 4361 (2004).
19. H. V. Herbert, *Z. Saugetierkd.* **50**, 141 (1985).
20. K. Ghose, C. F. Moss, *J. Acoust. Soc. Am.* **114**, 1120 (2003).
21. P. Dayan, L. F. Abbott, *Theoretical Neuroscience* (MIT Press, Cambridge, MA, 2001).
22. D. A. Butts, M. S. Goldman, *PLoS Biol.* **4**, e92 (2006).
23. A. Surlykke, K. Ghose, C. F. Moss, *J. Exp. Biol.* **212**, 1011 (2009).
24. T. Manabe, N. Suga, *J. Ostwald, Science* **200**, 339 (1978).
25. R. S. Heffner, G. Koay, H. E. Heffner, *J. Comp. Psychol.* **113**, 297 (1999).
26. M. Louis, T. Huber, R. Benton, T. P. Sakmar, L. B. Vosshall, *Nat. Neurosci.* **11**, 187 (2008).
27. N. S. Harper, D. McAlpine, *Nature* **430**, 682 (2004).
28. A. Brand, O. Behrend, T. Marquardt, D. McAlpine, B. Grothe, *Nature* **417**, 543 (2002).
29. D. McAlpine, D. Jiang, A. R. Palmer, *Nat. Neurosci.* **4**, 396 (2001).
30. We thank N. Sobel, J. Rubin, E. Simoni, A. Rubin, and N. Harper for comments on the manuscript; M. Holderied, I. Couzin, A. Arieli, E. Ahissar, and H.-U. Schnitzler for helpful discussions; and J. Barcelo for technical assistance. This study was funded by a Human Frontiers Science Program grant to N.U. and a Weizmann Institute Postdoctoral Fellowship to Y.Y.

Supporting Online Material

www.sciencemag.org/cgi/content/full/327/5966/701/DC1

Materials and Methods

SOM Text

Figs. S1 to S7

Movie S1

References

14 October 2009; accepted 23 December 2009

10.1126/science.1183310

Axon Extension Occurs Independently of Centrosomal Microtubule Nucleation

Michael Stiess,¹ Nicola Maghelli,² Lukas C. Kapitein,³ Susana Gomis-Rüth,¹ Michaela Wilsch-Bräuninger,² Casper C. Hoogenraad,³ Iva M. Tolić-Nørrelykke,² Frank Bradke^{1*}

Microtubules are polymeric protein structures and components of the cytoskeleton. Their dynamic polymerization is important for diverse cellular functions. The centrosome is the classical site of microtubule nucleation and is thought to be essential for axon growth and neuronal differentiation—processes that require microtubule assembly. We found that the centrosome loses its function as a microtubule organizing center during development of rodent hippocampal neurons. Axons still extended and regenerated through acentrosomal microtubule nucleation, and axons continued to grow after laser ablation of the centrosome in early neuronal development. Thus, decentralized microtubule assembly enables axon extension and regeneration, and, after axon initiation, acentrosomal microtubule nucleation arranges the cytoskeleton, which is the source of the sophisticated morphology of neurons.

The centrosome is regarded as the primary source of microtubules in axonal and dendritic growth (1, 2). It is thought that microtubules assemble at the centrosome, then are released and move along the axon through motor

proteins (1, 3, 4). Furthermore, in vitro the centrosome directs axon formation in vertebrate and invertebrate neurons (5, 6), but this has not been confirmed in vivo (7). Microtubules, however, can also assemble locally from subunits or

small oligomers within the axon (8–10). Indeed, flies that lose centrosomes during development seem to develop a largely normal nervous system, where the direction of axon outgrowth appears not to be affected (11). Thus, the role of the centrosome and centrosomal microtubule nucleation in axon growth is controversial (12–15).

To define the role of the centrosome in microtubule nucleation during neuronal development, we first determined where microtubules are nucleated during the development of rodent hippocampal neurons. Microtubules were depolymerized with nocodazole, and the microtubule nucleation sites were examined after washout of the drug (Fig. 1A). In young neurons that had just initiated an axon [2 days in vitro (DIV)], microtubules

¹Independent Junior Research Group Axonal Growth and Regeneration, Max Planck Institute of Neurobiology, Am Klopferspitz 18, 82152 Martinsried, Germany. ²Max Planck Institute of Molecular Cell Biology and Genetics, Pflotenhauerstrasse 108, 01307 Dresden, Germany. ³Department of Neuroscience, Erasmus Medical Center, Dr. Molewaterplein 50, 3015 GE Rotterdam, Netherlands.

*To whom correspondence should be addressed. E-mail: fbradke@neuro.mpg.de